Children's Hospital of Philadelphia

Annual Progress Report: 2005 Formula Grant

Reporting Period

July 1, 2009 – December 31, 2009

Formula Grant Overview

The Children's Hospital of Philadelphia received $3,460,487 in formula funds for the grant award period January 1, 2006 through December 31, 2009. Accomplishments for the reporting period are described below.

Research Project 1: Project Title and Purpose

Nerve Promoting Factors from the Early Embryonic Inner Ear - The cochlear implant is a remarkable electronic device that can restore hearing to profoundly deaf children. It works by bypassing the sound-sensitive tissues of the inner ear to provide direct electrical stimulation of the nerve of hearing, the auditory nerve. A child's success with a cochlear implant depends on maintaining auditory nerve cells, which can be diminished substantially by some forms of deafness. The purpose of this project is to characterize a critical nerve-stimulating substance called ODF, a mixture of unknown active proteins secreted by the inner ear during embryonic development. ODF has a powerful effect on nerve cell growth and survival, and so may have great clinical potential for stimulating nerve regeneration and possibly helping children perform better with cochlear implants.

Duration of Project

1/1/2006 - 12/31/2009

Project Overview

The development of the early auditory nerve, the cochleovestibular ganglion (CVG), depends on diffusible signals from the early embryonic inner ear (otocyst). One of the earliest of these signals is otocyst-derived factor (ODF), a poorly characterized substance secreted by the early inner ear. ODF causes exuberant outgrowth of nerve processes and promotes neuron survival, both in primitive neurons in the early CVG and in more mature auditory neurons in later development. The long-term objective of this project is to identify the active factor(s) in ODF and determine how they function in development. Approaching these questions will be greatly facilitated by the recent discovery of a functionally-identical neurotrophic activity secreted by cell lines derived from the mouse otocyst. This discovery should solve the problem that plagued the characterization of ODF in the past, that of the very limited quantity of material obtainable from the tiny otocyst. Ultimately, the investigators aim to apply the factor(s) present in ODF in

clinical practice, to reduce auditory nerve degeneration following deafness or even to regenerate the auditory nerve, both of which would improve cochlear implant performance in deaf children.

This project will measure the broad effects of ODF on neuron growth, survival, and gene expression in cultured CVG explants. Chick and mouse CVG tissues are harvested at various stages of development and exposed to cell-line derived ODF, and the responses compared with known neurotrophic factors. Genes whose transcription is up- or down-regulated by ODF will be identified by quantitative gene expression techniques, including expression microarray technology. The resulting data will help characterize the bioactivity of ODF throughout development, and will help to identify the signaling pathways activated downstream of ODF stimulation. The latter, in turn, should help the investigators generate hypotheses about the identity of the active factor(s) in ODF itself, to be tested in future extensions of this project.

Principal Investigator

John A. Germiller, MD, PhD
Children's Hospital of Philadelphia
Wood Center 1st Floor
34th St. & Civic Center Blvd.
Philadelphia, PA 19104

Other Participating Researchers

Charles Gawthrop, MD – employed by Children's Hospital of Philadelphia
Luv Javia, MD -- employed by Children's Hospital of Philadelphia

Expected Research Outcomes and Benefits

Expected outcomes: First, this research is expected to help identify the active protein factors in ODF, a recently-discovered substance that produces remarkable stimulation of the nerve of hearing, the auditory nerve. Even if it is unable to directly identify these active components, this project will produce extremely valuable information to target future research toward that goal. Second, it is expected to lead to a much better understanding of the effects of ODF on the auditory nerve throughout life, not just in the early stages of development in which it was discovered.

Expected benefits and improvement in health status: It is expected that one or more of the active factors in ODF may be potentially useful as therapeutic agents in patients affected by hearing loss. ODF stimulates tremendous growth and survival of auditory nerve cells. These nerve cells carry sound information from the inner ear to the brain, and are the sole target of stimulation by a cochlear implant, a remarkable device capable of restoring hearing to deaf individuals. In many forms of deafness, unfortunately, auditory nerve cells are lost in large numbers, which can jeopardize the success of this technology in affected patients. Therefore, it is critical that factors like ODF, which may reduce nerve loss or even regenerate nerve cells, be better developed and characterized. This project will help identify those factors in ODF most stimulatory for those nerve cells, which will be same ones most likely to stimulate nerve tissues if implanted into the

deaf inner ear. Therefore, this research will help identify agents that could be applied in the inner ear toward helping deaf children perform better with the cochlear implant.

Summary of Research Completed

Overview: During the reporting period, the researchers investigated a finding from their analysis of differentially expressed genes in expression microarrays. The researchers found several genes related to gamma-interferon signaling that were significantly upregulated after ODF exposure. Because the media used to grow the IMO-2B1, and the control media, contain gamma-IFN, the researchers investigated whether there was a difference in concentration of gIFN between experimental and control media. The researchers also tested whether adding exogenous gIFN, or a neutralizing antibody, affected neurotrophic activity of the ODF supernatants in bioassays. For the latter, chick cochleovestibular ganglion explants were used, as in prior experiments.

<u>Differential expression of gIFN-related genes by Microarray Analysis</u>
Using the microarray expression datasets from the last reporting period, the researchers calculated differential expression fold change for several genes related to gIFN. Raw microarray data were analyzed by computing the average fold change for the six comparisons (matched ODF-control pairs), the mean and standard deviation of the pair differences, then computing t and p-values by pairwise comparisons. Candidate genes were highlighted if fold change was statistically significant ($p<.05$ paired t-test) and greater than 1.5-fold in either direction.

The top 44 differentially expressed genes related to interferon signaling are shown in Table 1. Fold change ranges from 4.8 to 133. Well-represented genes include interferon-induced proteins, interferon regulatory factors, as well as GTPase and G-protein coupled signaling genes involved in interferon signaling. Tgtp, or T-cell specific GTPase, is a gamma-IFN induced gene and tops the list (133-fold upregulation).

Because gamma-IFN is added to the IMO-2B1 cell line media, the researcher postulated that these data may indicate there were differences in active gIFN levels between active and control supernatants. In our collaborator's lab, both media are routinely supplemented with equal amounts of recombinant gIFN. Therefore, the researcher compared control media and active supernatants for gIFN concentration using enzyme-linked immunosorbent assay (ELISA). Results are in Table 2. The IMO-2B1 conditioned media were found to have significantly higher concentrations of gIFN.

To determine whether this higher gIFN concentration caused the neurotrophic effects observed in earlier experiments, chick CVG explants were plated as before, and exposed to IMO conditioned media and control media, with or without the addition of recombinant gamma IFN or a gamma-IFN neutralizing antibody. Neurite outgrowth was scored at 24 and 48 hours. Results are in Figure 1. While there is still a large difference in neurite score between IMO-CM and control media, the addition of exogenous IFN or its antibody did not appear to affect neurite outgrowth substantially, for either condition. These data suggest that the gIFN is not the cause of the neurotrophic activity in the ODF supernatants (i.e., the IMO-2B1 conditioned media). Nevertheless, our collaborators (Dr. Barald and Bianchi) are investigating further whether gIFN

has any neurotrophic effects by itself, and in the future will be testing each active supernatant for gIFN concentration by immunoassays as well.

Gene Symbol	Fold Change	Gene Title
Tgtp	133.00	T-cell specific GTPase
Gbp4	87.85	guanylate nucleotide binding protein 4
Iigp1	85.28	interferon inducible GTPase 1
Gbp2	82.68	guanylate nucleotide binding protein 2
Gbp2	60.21	guanylate nucleotide binding protein 2
Mpa2l /// LOC626578 /// LOC673101	52.03	macrophage activation 2 like /// similar to macrophage activation 2 like /// similar to macrophage activation 2 like
LOC240327	39.66	Hypothetical LOC240327
Ifi203	36.77	interferon activated gene 203
AI451557	35.10	expressed sequence AI451557
LOC630509 /// LOC674192	33.58	similar to H-2 class I histocompatibility antigen, Q7 alpha chain precursor (QA-2 antigen) /// region containing histocompatibility 2, Q region locus 9; histocompatibility 2, Q region locus 7
Iigp2	25.93	interferon inducible GTPase 2
Igtp	23.06	interferon gamma induced GTPase
Psmb8	22.96	proteosome (prosome, macropain) subunit, beta type 8 (large multifunctional peptidase 7)
5830443L24Rik /// LOC626578	21.93	RIKEN cDNA 5830443L24 gene /// similar to macrophage activation 2 like
Rtp4	20.42	receptor transporter protein 4
Iigp1	19.62	interferon inducible GTPase 1
Cxcl9	19.36	chemokine (C-X-C motif) ligand 9
Ifi47	19.04	interferon gamma inducible protein 47
9830147J24Rik	18.37	RIKEN cDNA 9830147J24 gene
Tap1	18.17	transporter 1, ATP-binding cassette, sub-family B (MDR/TAP)
Serpina3g	18.12	serine (or cysteine) peptidase inhibitor, clade A, member 3G
9830147J24Rik	15.44	RIKEN cDNA 9830147J24 gene
Psmb9	14.90	proteosome (prosome, macropain) subunit, beta type 9 (large multifunctional peptidase 2)
Stat1	13.97	signal transducer and activator of transcription 1
Ifi205 /// Mnda	12.85	interferon activated gene 205 /// myeloid cell nuclear differentiation antigen
H2-T23 /// C920025E04Rik /// LOC667803 /// LOC672711 /// LOC674134	12.70	histocompatibility 2, T region locus 23 /// RIKEN cDNA C920025E04 gene /// similar to H-2 class I histocompatibility antigen, D-37 alpha chain precursor /// similar to H-2 class I histocompatibility antigen, D-37 alpha chain precursor /// similar to H-2 c
Irf8	12.25	interferon regulatory factor 8
H2-D1 /// H2-K1 /// LOC56628	12.07	histocompatibility 2, D region locus 1 /// histocompatibility 2, K1, K region /// MHC (A.CA/J(H-2K-f) class I antigen
H2-K1	9.94	histocompatibility 2, K1, K region
Oasl2	9.52	2'-5' oligoadenylate synthetase-like 2
Tap2	9.24	transporter 2, ATP-binding cassette, sub-family B (MDR/TAP)
Plec1 /// LOC671535	8.30	plectin 1 /// similar to poly (ADP-ribose) polymerase family, member 10
Ly6a	8.04	lymphocyte antigen 6 complex, locus A
Ifit1	7.70	interferon-induced protein with tetratricopeptide repeats 1
Casp12	7.39	caspase 12
Irf8	7.14	interferon regulatory factor 8
Psmb10	6.89	proteasome (prosome, macropain) subunit, beta type 10
Gvin1	6.47	GTPase, very large interferon inducible 1
Arts1	6.26	type 1 tumor necrosis factor receptor shedding aminopeptidase regulator
Irf1	6.05	interferon regulatory factor 1
Arts1	5.72	type 1 tumor necrosis factor receptor shedding aminopeptidase regulator
Stat1	5.42	signal transducer and activator of transcription 1
Ifi35	5.12	interferon-induced protein 35
Ifi35	4.83	interferon-induced protein 35

Table 1. Differential Gene expression of gamma-interferon (gIFN)-related genes. Dissociated neonatal spiral ganglion neurons were grown as 6 matched pairs – ODF vs. control media, and cDNA hybridized with Affymetrix mouse genome expression arrays. Results are listed in order of fold-change between IMO-conditioned media and control media. All were upregulated genes.

Sample	Type	IFN-γ (pg/mL)
D	Active IMO-2B1 CM	3368.6
2	Active IMO-2B1 CM	1617.5
3	Active IMO-2B1 CM	1615.8
1	Active IMO-2B1 CM	1209.7
4	Active IMO-2B1 CM	1150.6
14	Active IMO-2B1 CM	808.7
6	Active IMO-2B1 CM	284.7
11	Control media	35.2
10	Control media	14.6
7	Control media	0.0
8	Control media	0.0
9	Control media	0.0
13	Control media	0.0
15	Control media	0.0
E	Control media	0.0
A		0.0
B		0.0

Table 2. Gamma-interferon concentrations of the conditioned and control media, as determined by ELISA.

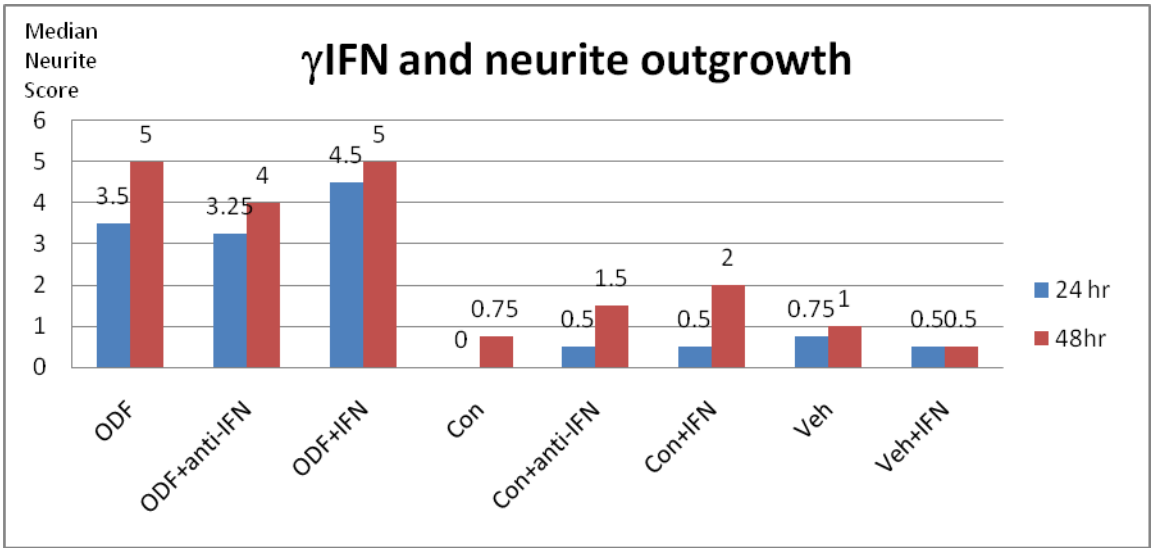

Figure 1. Effect of gIFN, or gIFN-neutralizing antibody, on neurite outgrowth in chick embryo CVG explants. Neurite scores reflect the median from N=5 explants per datapoint. While a large difference is still observed between experimental conditioned media and control media, the addition of exogenous gIFN or a neutralizing antibody did not appreciably affect the results. Con, control media. Veh, vehicle.

Research Project 2: Project Title and Purpose

Functional Imaging in 4 Dimensions: Magnetoencephalography (MEG) - Detection and recording of brain functional activity using MEG offers unique advantages over alternative methodologies (such as positron emission tomography and functional magnetic resonance imaging). In particular, MEG offers direct non-invasive recording of neuronal activity with sub-millisecond temporal resolution and no radiation risk. Consequently, both neuronal activity evoked by a stimulus presentation or by cognitive or motor task performance, as well as spontaneous activity can be recorded. This project is to explore the fine structure of evoked responses detected by MEG, and to define temporal signatures of normal and abnormal brain function, with a view to definition of electrophysiological phenotypes of developmental disorders such as autism, ADHD and learning disability.

Duration of Project

1/1/2006 - 12/31/2009

Project Overview

The overall goal of this project is to explore in children the time-domain of functional brain activity via non-invasive MEG recording. While many functional imaging approaches adopt a "locationalist" perspective, focusing on the spatial organization of functional centers in the brain, MEG offers a real-time methodology for recording the fine temporal structure of neuronal electrical activity. Specifically, the high temporal resolution recording offers the opportunity to explore stimulus information encoding in the latency shifts of specific evoked response components (measured on a millisecond scale). It also offers the opportunity to record endogenous or elicited rhythmic activity in characteristic frequency bands. In particular, activity in the gamma band (~40Hz) has been speculatively associated with cognitive functions. Temporal resolution of the order of a few milliseconds is necessary to adequately characterize modulations (amplitude and frequency shifts) of such activity. Recently, streams of research have suggested that physical attributes of auditory stimuli (such as their frequency and intensity) may be reflected in latency variations of the evoked response component detected by MEG approximately 100ms post stimulus onset. The first aim of the project is to model the latency behavior of 50ms and 100ms components of the auditory evoked neuromagnetic field in children as a function of stimulus acoustic properties, perceptual classification, immediate context (preceding stimuli), and as a function of developmental age. Finely grained stimuli of increasing spectral complexity and linguistic character (including isolated vowels and vowel-consonant, VC, combinations) will systematically probe auditory and early speech processing at the level of auditory cortex. The second aim is to identify attributes of the temporal response to such stimuli that serve as "temporal signatures" of abnormal auditory and speech processing, by examining children with diagnoses of language impairment (including autism spectrum disorders, ADHD and learning disability). The third aim is to identify rhythmic activity in the gamma band (~40Hz) occurring in sensory cortex during attentional states. In particular, it is a goal to document modulation of gamma band activity within a particular sensory cortex (e.g. auditory vs. visual) during selective attention towards and away from that sensory modality. The fourth

aim is to quantify abnormalities in such gamma band intensity modulation in patients with attentional abnormalities (including autism spectrum disorders, ADHD and learning disability).

Principal Investigator

Timothy P.L. Roberts, PhD
Children's Hospital of Philadelphia
34th Street and Civic Center Blvd.
2nd Floor, Wood Building
Philadelphia, PA 19004

Other Participating Researchers

J.C.Edgar, PhD, M. Ashtari, PhD, W. Gaetz, PhD, D. Zarnow, MD, E. Schwartz, MD,
T. Lei, PhD – employed by Children's Hospital of Philadelphia

Expected Research Outcomes and Benefits

A basic goal of functional brain imaging is to identify neural correlates of behavior, i.e., activity in the brain associated with performance in the world. We will derive a model of the observable neural correlates of key processes of sound and speech perception and processing that we use to identify features such as pitch, spectral quality and, in the case of speech perception, vowel identity. As such, this will provide basic neuroscientific understanding of the early processes in brain, associated with the transformation of "heard sound" into "perceived music, or speech". Deviations from this model in populations of children with language impairment may provide (1) a basic understanding of the origins of language impairment, as a potential consequence of abnormal early sound processing in the brain, (2) objective (potentially diagnostic) indices of processing abnormalities, predictive of subsequent impaired language function, (3) markers for patient stratification for treatment according to the area of the brain, and level of stimulus complexity, at which deviations from normal processing are observable, (4) non-invasive monitoring of potential therapeutic response. Additionally, these "temporal signatures" of abnormal brain function may serve as characteristic features (sometimes referred to as "electrophysiological endophenotypes"), which may more specifically describe the brain activity in disorders such as autism. These might thereby inform experimental model development based on research in genetics, more tightly coupling bench and bedside endeavors. Similarly, quantification of changes in a certain (gamma-band) brain rhythm may provide an objective and quantitative index of attention. Deficiencies or absence of these changes in children with attentional difficulties may represent neural correlates of this behavioral symptom, again offering objective, quantifiable measures as well as a basic neuroscientific interpretation. Overall, the emphasis of this project is on exploiting the high temporal resolution recording of brain activity provided by MEG to understand language and attention difficulties in children with developmental disorders.

Summary of Research Completed

1. Subject Recruitment

During the course of this 6 month period, 7/1/2009-12/31/2009, a total of 42 children and 18 adults with diagnoses of autism, Asperger disorder, specific language impairment (SLI), schizophrenia, Parkinson's disease or healthy control subjects were recruited and underwent MEG scanning on a range of protocols investigating endogenous rhythmic activity, auditory processing, face processing, attention and language. One of the expected outcomes of this grant, which was to establish a research program in MEG at the Children's Hospital of Philadelphia, has clearly been achieved.

2. Clinical assessment

Each pediatric subject was evaluated by a dedicated neuropsychologist (Dr Blaskey, Dr Woldorff, or Dr Hernandez) and underwent evaluation of IQ, language function (CELF-4 and CASL), autism (ADOS, SCQ, SRS) and other assessments. A strength of the program, in its endeavor to identify neural correlates of disorders such as autism, is the rigorous and extensive behavioral testing and clinical and neuropsychological evaluation.

3. Research Accomplishments

Since the program has been successful in attracting significant extramural support for many of the studies relating to auditory processing in autism spectrum disorders, leveraging in part the accomplishments under this program, this report will focus on the innovative pilot endeavors that will likely form the basis for subsequent directions of laboratory inquiry, and funding.

<u>The Fusiform Face Response: explicit vs. implicit processing of emotion</u>

The fusiform face area (FFA) responds preferentially to faces over other classes of visual stimuli, however, it is unclear whether emotional face information modulates early FFA activity. Seventeen healthy adults viewed emotionally expressive faces and were instructed to make a button response based on age (young, middle-aged, older; implicit condition) or emotion (fearful, happy, neutral; explicit condition) during acquisition of 275-channel whole-head magneto-encephalography (MEG). Dipole source modeling with regional sources produced source waveforms for localized left and right primary visual and fusiform activity. Stronger left M170 FFA activity to fearful than happy or neutral faces was observed in the explicit task, while amplitude differences were not seen in the implicit task. A main effect of emotion was seen for later M230 FFA amplitude, greatest to fearful faces. Interestingly, a strong association between greater early fusiform activity and faster behavioral reaction times in the explicit task provides supporting evidence for the role of the fusiform gyrus in processing emotional information.

Higher association cortices as well as unisensory areas can support multisensory integration (Senkowski et al., Trends in Neuroscience, 31, 401-409, 2008). The present study investigated whether audiovisual integration of emotional information emerges early at unisensory or later at higher association cortices. Emotional stimuli were presented in three blocks (audiovisual (AV),

auditory (A), visual (V)). Eighteen participants performed a delayed emotional recognition task (happy, angry, or neutral prosody and/or facial expression) while whole-brain magnetoencephalography (MEG) data was obtained. Time-frequency evoked and total power analyses were performed on the sensor data, and source localization of the frequencies of interest performed via SAM beamformer. To examine crossmodal integration between bimodal and unimodal conditions, two contrasts were specified: AV > A and AV > V. In the AV > A contrast, early evoked responses were observed for both temporal and occipital cortices. However, at the source level, early alpha desynchronization was observed only in occipital cortex, with no changes in temporal cortices. In the AV > V contrast, findings from both sensor and source levels revealed increased alpha desynchronization only in temporal cortices, with no changes in visual cortex. Thus, no crossmodal effect in unisensory areas emerged. Instead, increased frontal alpha activity in both the AV > A and AV > V contrasts supports the view that affective information from face and prosody converges at higher association cortices.

Age predicts visual gamma oscillation frequency (in collaboration with CUBRIC, Department of Psychology, Cardiff, UK)

There is increasing interest in gamma oscillations (> 40 Hz) as an index of visual information processing. Recent reports have shown considerable inter-individual variability of induced gamma oscillation frequency and amplitude yet the underlying factors behind this variability are unclear. The purpose of the current study was to examine how gamma frequency and amplitude cortical measures relate to basic between subject factors such as age. Participants (N=44) ranged in age from 10 to 46 yrs (mean of 30.3 yrs). Stimuli consisted of vertical, stationary, maximum contrast, three cycles per degree, square-wave gratings presented on a mean luminance background. Stimuli were presented in the lower left visual field and subtended 4° both horizontally and vertically, with the upper right corner of the stimulus located 0.5° horizontally and vertically from a small red fixation cross. Participants were instructed to fixate for the entire experiment and to press a response key with the right index finger at the termination of each stimulation period (varying in duration 1.5 to 2 seconds). MEG data was first analyzed using synthetic aperture magnetometry (SAM) and then by performing time-frequency analysis of SAM source waveforms at SAM peak locations from right primary visual cortices.

Consistent with previous findings, gamma oscillations show considerable inter-individual variability in terms of frequency, and amplitude. However, our results demonstrate a significant negative correlation between the observed gamma oscillation frequency and the participant's age ($r^2 = -0.46$, $p < 0.0005$). A recent report assessing both MEG visual gamma and MRS GABA indicate that gamma frequency is also correlated with GABA concentration. Thus, the reduction of visual gamma frequency may be in part due to the known decrease of GABA with increasing age.

GABA and Gamma: GABA MRS correlates with Gamma Oscillations recorded with MEG in Visual and Motor Cortex

Animal and non-invasive human pharmacological studies demonstrate a relationship between cortical neural oscillations and the inhibitory neurotransmitter γ-Amino butyric acid (GABA). The present study compared visual and motor cortex gamma oscillatory activity (~40 to 90 Hz),

detected with MEG, with each subject's level of GABA in visual and motor areas, detected with magnetic resonance spectroscopy (MRS).

Eight healthy adult control subjects participated (3F, 22-45 years). Each subject underwent MEG with visual and motor paradigms designed to elicit gamma oscillations in primary sensory cortex. MEG data was recorded using a 275-channel biomagnetometer (VSM Medtech). To identify motor cortex gamma activity, participants made button responses using their right-index finger in response to a change in the color of a visually presented fixation cross. Peri-movement gamma activity was estimated by localizing contralateral motor cortex using a differential beamformer, and then source waveforms from the peak event-related desynchronization (ERD) location (15-30Hz) were used to estimate peri-movement gamma-band power (65-90Hz). For visual cortex, a small grating stimuli was displayed in the lower-left quadrant of the visual field, and subjects responded via a button press when the grating disappeared. Similar to motor gamma activity, visual gamma activity was assessed from the beamformer localized source waveform. In a separate exam, single voxel (30x30x30mm) GABA MRS was obtained using the MEGAPRESS spectral editing sequence2, with TE=68ms at 3T (acquisition time < 13'). MRS voxels were placed based on anatomic consideration, centered on the "hand-knob" of the left central sulcus for motor areas, and in the calcarine cortex for visual areas. Local highorder shimming allowed FWHM line-widths <10Hz for the unsuppressed water peak. After Fourier transformation, phase correction was applied to the un-subtracted spectra (on the Cr resonance) and propagated to the subtracted spectrum. The integral under the GABA resonance (at 3ppm) was obtained by spectral peak-fitting using a Gaussian resonance. A reference phantom of 50mM GABA was placed in the head coil with the subject and was also interrogated (using a 14x14x30mm voxel). GABA levels were estimated as the ratio of the cortical GABA integral to that of the phantom, and also with respect to an internal cortical reference NAA resonance at 2ppm. Associations were tested using linear regression in SPSS 16.0. GABA levels (whether quantified with respect to internal NAA or to the 50mM phantom) were clearly resolved and measured in all subjects in visual and motor regions of interest (ROIs). A negative association of GABA level with age was observed for visual and motor cortex ($r=-0.76$, $p<0.05$; $r=-0.88$, $p<0.01$, Fig. 2). Similarly, gamma-band activity (e.g. Fig. 1 right) was determined in all subjects (with the exception of the visual cortex in a single subject). The center frequency of gamma oscillations also showed a negative association with age for both primary sensory cortices ($r= -0.53$; $r= -0.59$). Furthermore, GABA levels and gamma frequency were positively associated in both primary sensory cortices ($r=0.52$; $r=0.69$, $p=0.056$, Fig. 3).

GABA levels and gamma band activity can be resolved and localized to motor and visual cortices. Both decline with increasing age. Furthermore, GABA levels correlate positively with gamma frequency for each cortical ROI. This suggests a multimodal neurobiological probe of brain function at the neurotransmitter and electrophysiological level. Present findings also provide support for a role of GABA in the generation and modulation of endogenous rhythmic brain activity.

Figures

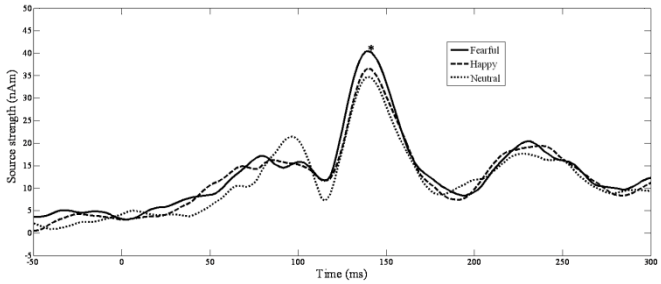

Fig 1: Left-hemisphere FFA grand average source waveforms for the fearful, happy, and neutral conditions (explicit task). Early fusiform source strength was stronger to fearful than happy or neutral faces ($p < 0.05$). To create the above plot, each individual's early FFA response was temporally shifted to be centered at the grand average M170 latency (~140 ms).

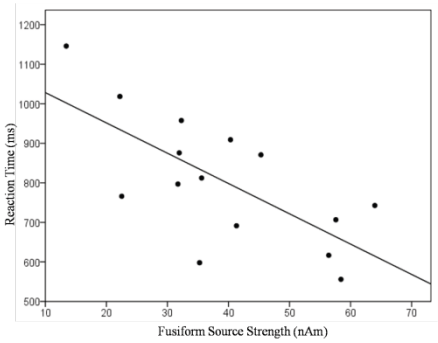

Figure 2: Zero-order correlation between early fusiform source strength and RT, collapsed across hemisphere. The strong association ($R^2 = 0.48$), accounting for nearly 50% of the RT variance, indicates the involvement of the fusiform gyri in explicit emotion processing.

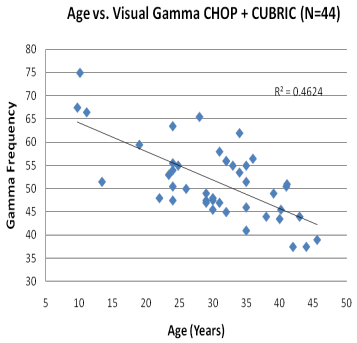

Fig 3: Results demonstrate a significant negative correlation between the observed gamma oscillation frequency and the participant's age ($r^2 = -0.46$, $p < 0.0005$)

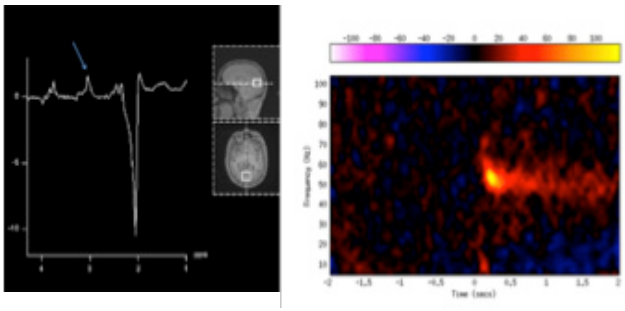

Fig. 4 (left) edited spectrum showing GABA resonance (arrow), obtained from occipital cortex voxel; (right) time-frequency spectrogram from MEG detected visual cortex activity during visual gating task. Peak gamma activity is identified by hottest color.

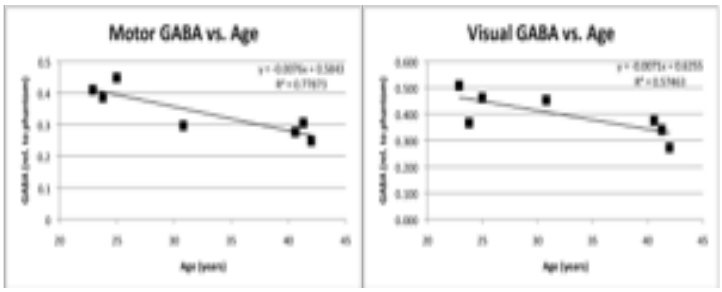

Fig. 5 GABA levels are negatively associated with age in both motor (left, $p<0.01$) and visual (right, $p<0.05$) cortex.

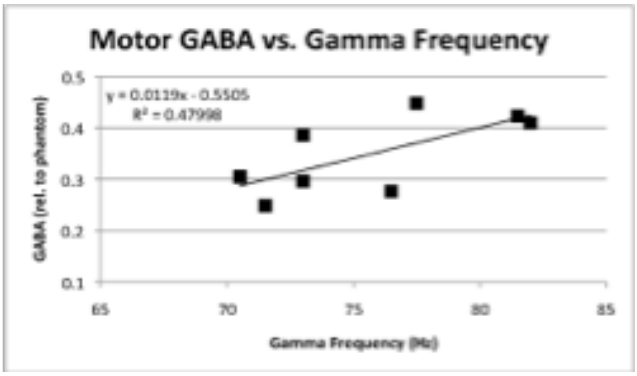

Fig. 6 positive association (p=0.056) between GABA levels and peak gamma-band frequency in motor cortex.

Research Infrastructure Project 3: Project Title and Purpose

Building a Multimodality Imaging Core Resource - The goal of this research infrastructure project is to develop a multi-modality experimental animal imaging resource to support, expand and extend the preclinical research investigations of a large number of CHOP investigators as well as to develop and refine an integrated translational research effort, which will allow ready translation of experimental and preclinical advances to the clinical setting. To achieve this goal, we are customizing space within the rodent facility, acquiring state-of-the-art imaging equipment (both of these aspects of the project are being supported by institutional funds), optimizing the state-of-the-art experimental animal imaging protocols (including microMRI, microCT and microPET) and establishing a common image post-processing and quantitative analysis endeavor, sharing and expanding resources of clinical radiology.

Duration of Project

1/1/2007 - 12/31/2009

Project Overview

Imaging is becoming central to experimental research involving laboratory animals. As advances in genetics and molecular biology offer an exponentially increasing number of possibilities for investigating and understanding the underlying biology of disease and therapeutic approaches, it becomes critical to evaluate new experimental models and treatments in an in-vivo setting. Advances in magnetic resonance imaging, in particular, offer the possibility of physiologically-specific and, most importantly, non-invasive assessment of disease progression and response. Thus, imaging can be viewed as a form of non-invasive histology, providing a quantitative and specific assessment of disease and treatment, without requiring the sacrifice of the animal. Not only that, it offers the valuable possibility of studying disease progression and response in individual animals, which (i) massively reduces the number of laboratory animals required to complete a study, and (ii) offers insights into the specific characteristics of atypical or non-responding individuals, more faithfully mimicking the clinical scenario.

To provide small animal imaging resources to the CHOP community requires the completion of the following specific aims:
(1) to select and commission imaging modalities to meet the needs of the CHOP research community;
(2) to develop and enhance physiologically-specific magnetic resonance imaging technologies, to more accurately and specifically address specific biological questions posed by the CHOP research community (e.g. to increase sensitivity to early signs of disease as an assessment of model penetrance, to improve the physiological interpretability of imaging findings in terms of biological quantities, such as “metabolism”, “vascularity”, “cellularity” and “angiogenesis”);
(3) to develop and enhance surrogate markers of treatment response, in the form of sensitive indicators of biologically activity of putative new treatments, such as antiangiogenic pharmaceuticals, where traditional preclinical endpoints may not be appropriate;
(4) to educate and inform the laboratory animal researchers at CHOP of the possibilities and capabilities of non-invasive imaging, with a view to increasing their utilization of the

technology, to reduce animal numbers required and to follow disease progression and response to therapy.

Principal Investigator

Timothy P.L. Roberts, PhD
Children's Hospital of Philadelphia
34th Street and Civic Center Blvd.
2nd Floor, Wood Building
Philadelphia, PA 19004

Other Participating Researchers

Suzanne Wehrli, MD, Roberto Accorsi, MD - employed by Children's Hospital of Philadelphia

Expected Research Outcomes and Benefits

Approximately 80% of the laboratory-based researchers at CHOP use one or more animal models in their research. Many rely on breeding large cohorts of "similar" animals for serial sacrifice and post-mortem assessment of the progression of disease. It is anticipated that the vast majority of these investigators would be able to benefit from the use of non-invasive imaging in their research: to (1) perform longitudinal or serial investigations, without the need to sacrifice animals at each "timepoint"; (2) to study individual disease progression and response in individual animals (for example, to identify characteristics predisposing individuals to particular progressions or responses); (3) to more directly relate their findings to clinical settings (where analogous imaging techniques are used in clinical radiology); and consequently (4) to speed up the progression from preclinical research to clinical trials of emerging new therapies.

Summary of Research Completed

The infrastructure for imaging small animals at the Children's Hospital of Philadelphia is now completely installed, and includes state of the art instrumentation in multiple modalities: MRI, CT, PET, SPECT, optical and ultrasound. Projects are underway, supporting the biological research of an increasing number of CHOP investigators.

A summary of projects and progress thereon is offered below:

Magnetic Resonance Imaging

Project: Effect of traumatic brain injury on ventricular size and morphology.

Measurement of ventricular volume		
- Live control	12 mice	14 studies
Test measurement of flow		
- Live control	6 mice	6 studies
Longitudinal mouse brain imaging post traumatic injury		
- Live mouse post brain injury	2 mice	4 studies

Project: Longitudinal in vivo imaging of mouse medulloblastoma, tumor progression, tumor regression during treatment with Hedgehog antagonist, recurrence of tumor and comparison with age matched controls.

- Live mouse longitudinal imaging 57 mice 369 studies

Project: Modeling children's brain tumors in mice: Snf5 is required for neurodevelopment. A study of myelination using Diffusion Tensor Imaging.

- Live mouse longitudinal imaging 39 mice 127 studies

Project: Immunotherapy: Development of Leukemia and Lymphoma in mice using mesenchymal stromal cells as drug delivery vehicle: Detection of abdominal tumors and measurement of the spleen size.

- Live mouse imaging of abdomen 51 mice 63 studies

Optical Imaging

The IVIS system was installed early 2009. The company Caliper Life Sciences gave us a one week basic training in February 2009 and another 1 week high level training will be given in February 2010.

Project: Adoptive immunotherapy for CD19-positive Leukemia using chimeric immunoreceptors **.**
Total number of mice for luminescence: 180 (imaged 5 times each)
Total number of mice for fluorescence: 6

Project: In utero gene therapy.
Total number of mice for luminescence: 20
Total number of mice for fluorescence: 0

Project: Hedgehog pathway inhibition in young mice results in severe bone defects.
Total number of mice for luminescence: 31
Total number of mice for fluorescence: 0

Project: Immunotherapy: Development of leukemia and lymphoma in mice using mesenchymal stromal cells as drug delivery vehicle.
Total number of mice for luminescence: 58 (imaged 4 times)
Total number of mice for fluorescence: 0

Project: Biology and therapy of neuroblastoma.
Total number of mice for luminescence: 14
Total number of mice for fluorescence: 0

Project: Feasibility of using Mir-34a as Therapy of neuroblastoma.
Total number of mice for luminescence: 98
Total number of mice for fluorescence: 0

Project: Characterization of Heme-Oxygenase-1 promoter under oxidant stress.
Total number of mice for luminescence: 8 litters (50 neonatal mice)
Total number of mice for fluorescence: 0

UltraSound Imaging

The Visual Sonics VEVO system was installed in 2009. The vendor-company VisualSonic gave us a 1-week basic training in March 2009 and another 1 week high level training during the summer of 2009. In the last 6 months, the following studies have been initiated:

Project: In utero gene therapy.
Total number of pregnant mice: 144
Total number of US guided injection in embryos: 576

Project: Polyamine inhibition blocks initiation and progression of neuroblastoma. Detection and measurement of the size of Neuroblastoma tumors using US.
Total number of TH_MYCN mice: 114

Project: MicroRNA function in lung development. US guided injection of lenti-viral vector for microRNA overexpression in E14 mouse fetal lung.
Total number of pregnant mice: 15
Total number of US guided injection in embryos: 70

Project: Fetal Gene Therapy: US guided injection of lentiviral vetor into fetal pups.
Total number of pregnant mice: 30
Total number of US guided injection in embryos: 270

Project: Fetal Gene Therapy: US guided injection of cells into the amniotic cavity for the cure of myelomeningocele.
Total number of pregnant rats: 10
Total number of US guided injection in embryos: 150